



ELSEVIER

Available online at [www.sciencedirect.com](http://www.sciencedirect.com)

SCIENCE @ DIRECT®

Nuclear Instruments and Methods in Physics Research A 508 (2003) 388–393

**NUCLEAR  
INSTRUMENTS  
& METHODS  
IN PHYSICS  
RESEARCH**  
Section A[www.elsevier.com/locate/nima](http://www.elsevier.com/locate/nima)

# Performance of a large-area avalanche photodiode at low temperature for scintillation detection

L. Yang<sup>a,\*</sup>, S.N. Dzhosyuk<sup>a</sup>, J.M. Gabrielse<sup>a,1</sup>, P.R. Huffman<sup>a,b</sup>, C.E.H. Mattoni<sup>a</sup>,  
S.E. Maxwell<sup>a</sup>, D.N. McKinsey<sup>a,2</sup>, J.M. Doyle<sup>a</sup>

<sup>a</sup> Department of Physics, Harvard University, Cambridge, MA 02138, USA

<sup>b</sup> National Institute of Standards and Technology, Gaithersburg, MD 20899, USA

Received 24 February 2003; accepted 11 April 2003

## Abstract

We investigate the performance of a large-area (13 mm × 13 mm) avalanche photodiode at temperatures ranging from 4.2 to 77 K. We find that the gain, at a given bias voltage, increases with decreasing temperature down to 40 K, below which a premature breakdown phenomenon occurs. The quantum efficiency of the device decreases with decreasing temperature until approximately 40 K, at which point it drops abruptly to <15% of its room temperature value. The sensitivity of the device above 40 K makes it a good candidate for detection of scintillation light in low-temperature systems.

© 2003 Elsevier B.V. All rights reserved.

PACS: 07.60.Dq; 29.40.Mc; 29.40.Wk

Keywords: Scintillation detection; Avalanche photodiode; Quantum efficiency; Low temperature; Carrier freeze-out

## 1. Introduction

Detection of scintillation light is a common and important method used to characterize elementary particle decay. For example, in an experiment to measure the lifetime of a free neutron [1,2], neutrons are confined in a bath of superfluid helium by a large magnetic field and scintillations

are produced in the helium when the neutrons undergo beta decay. The ideal detector for such a system would be one that could operate at low temperatures (in or near the helium bath) and high magnetic fields ( $\approx 1$  T). At present, the commonly available photomultiplier tube (PMT) is used. PMTs however cannot, in general, be operated in high fields or at low temperatures. Thus, the PMTs used in the lifetime experiment must be placed at a significant distance from the helium bath, thereby reducing the overall light detection efficiency.

Compared to PMTs, large-area silicon avalanche photodiodes (APDs) have higher noise, lower gain and higher cost per unit area. Nevertheless, their high immunity to magnetic fields (due to the short path traversed by charge carriers),

\*Corresponding author. NIST, Bldg. 235, room B183, 100 Bureau Drive, Mail Stop 8461, Gaithersburg, MD 20899-8461, USA.

E-mail address: [liang@jsbach.harvard.edu](mailto:liang@jsbach.harvard.edu) (L. Yang).

<sup>1</sup> Current address: Calvin College, Grand Rapids, MI 49546, USA.

<sup>2</sup> Current address: Princeton University, Princeton, NJ 08544, USA.

high quantum efficiency, and compact size make them an attractive alternative to PMTs in some applications. APDs have been studied for liquid xenon scintillation detection down to 168 K [3,4] and for photon counting at 100 and 85 K [5,6]. However, their performance at lower temperatures is not fully characterized. In this work, we set out to find the temperature range at which APDs can be operated and investigate certain noise properties of the device at low temperatures. We also investigate the key parameters that impact on the suitability of the APD for detecting neutrons in the neutron lifetime experiment.

## 2. Experimental apparatus

In our tests, an APD is held in a liquid helium cryostat. The cylindrical cryostat allows both room temperature access and radial optical access (see Fig. 1). The APD is mounted using a Teflon collar onto a copper plate that is thermally

anchored to the inner wall of the helium bath using beryllium-copper spring fingers. The temperature of the copper anchor can be controlled using a 1 k $\Omega$  heater mounted alongside the APD. The temperature is monitored using a diode thermometer<sup>3</sup> that is mounted to the copper plate. During cooldowns, helium buffer gas (which provides a direct thermal contact between the APD and the walls of the liquid helium bath) is often introduced into the vacuum chamber to reduce the cooldown time. Before biasing the APD, however, the pressure in the inner vacuum chamber must be reduced to below 13 Pa (0.1 Torr) to prevent discharges between the APD high-voltage lead and ground, which would destroy the charge preamplifier.

The signal from the APD is transported to room temperature using a cryogenic semi-rigid co-axial cable chosen to minimize heat load.<sup>4</sup> The signal is amplified with a charge sensitive preamplifier<sup>5</sup> and then with a spectroscopy amplifier. The spectroscopy amplifier has a 1  $\mu$ s shaping time, with the output fed into either a 2048 channel multi-channel analyzer (MCA) or a digital oscilloscope.

In all of our tests, the APD is operated in the gain mode (below breakdown regime), with a reverse bias below 1800 V at room temperature, and lower voltages at lower temperatures. (For example, at 77 K, the breakdown voltage of the particular APD we tested dropped to 1390 V.) A 10 M $\Omega$  resistor in series with the APD (see Fig. 1) limits the current at breakdown to prevent damage to the APD and other electronics.

The sources used to test the APD are an <sup>55</sup>Fe source that produces 5.9 keV X-rays and a red light emitting diode (LED) that emits 0.5  $\mu$ s long light pulses with a repetition rate of 1–8 kHz. The

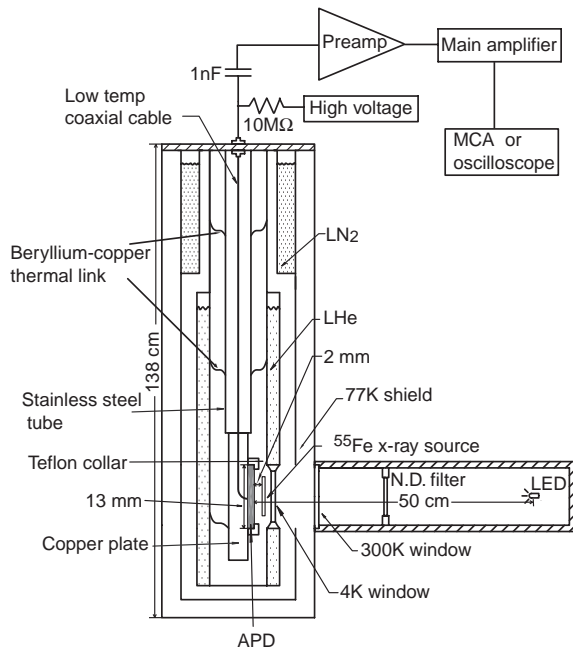


Fig. 1. A schematic of the liquid helium dewar used in these measurements (not to scale). The components are discussed in the text.

<sup>3</sup> Lakeshore model DT-470 diode thermometer. Certain trade names and company products are mentioned in the text or identified in illustrations in order to adequately specify the experimental procedure and equipment used. In no case does such identification imply recommendation or endorsement by the National Institute of Standards and Technology, nor does it imply that the products are necessarily the best available for the purpose.

<sup>4</sup> Oxford Instruments cryogenic feed and superconductive 50  $\Omega$  semi-rigid co-axial cable.

<sup>5</sup> Amptek A250 charge sensitive preamplifier with InterFET IF1801 input FET.

X-ray source is placed 2 mm away from the APD and the LED sits 50 cm away inside a light-tight aluminum can (see Fig. 1).

### 3. Device characterization

#### 3.1. Gain

To characterize the gain of the APD, the device is initially set to a reverse bias of 200 V. At this voltage, the electric field in the depletion region is insufficient to cause carrier multiplication<sup>6</sup>; the output signal in fact varies less than 10% for reverse bias voltages between 100 and 300 V. The intensity of the red LED and the gain of the spectroscopy amplifier are adjusted to produce an easily readable pulse height on the oscilloscope (approximately 22,000 photoelectrons). The reverse bias voltage is then raised and the pulse height at a given voltage is recorded. The ratio of this value to the pulse height at 200 V determines the gain at that voltage. To avoid saturation of the amplifiers at higher gains, the light from the LED must be attenuated. This is done by lowering the bias voltage on the LED. To accommodate the change in intensity incident on the APD, two measurements are taken at a fixed APD gain—one measurement for each intensity—and a scaling factor is calculated to relate the data taken at the different intensities.

Measurements of the gain as a function of the reverse bias voltage were taken at 300, 77, 40, and 14 K. This data are shown in Fig. 2. At 300 K, the APD we tested reached maximum gain of  $10^3$ . Measurements at 77 K show an enhancement in gain at a fixed voltage, consistent with that reported in Ref. [5]. We also see a continued steepening of the gain versus voltage curve at 40 K.

The dependance of the gain on temperature and reverse bias voltage does not agree with the model given in Ref. [3]. In that model, the gain is taken to be a function of the “effective voltage”,  $V_{\text{eff}} = V_{\text{applied}} - \alpha T$ , where  $\alpha$  is a constant and  $T$  is the temperature. The authors show that their data

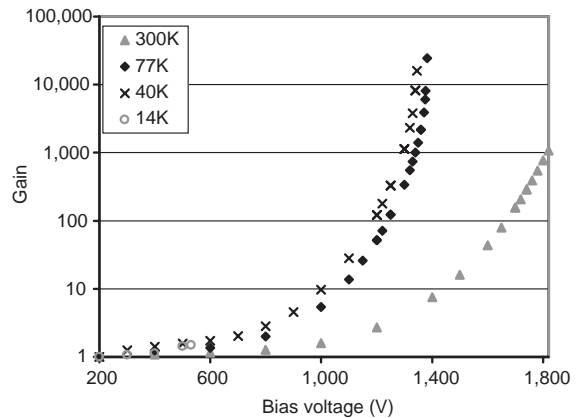


Fig. 2. Measurements of the gain of the APD as a function of the reverse bias voltage for four temperatures. Experimental conditions are described in the text.

between 170 and 300 K agree well with the model. However, our measurements show that this linear model is insufficient for the 14–77 K temperature range.

Below 40 K, the apparent onset of breakdown (as determined by observing the preamplifier output) is observed at a much lower bias voltage. At 14 K, this breakdown behavior appears at a reverse bias of 500 V. Note that the current through the APD during these “apparent breakdowns” was not measured and thus one cannot definitively conclude that they are avalanche breakdowns. The apparent breakdown lasts until the reverse bias voltage is set to low voltage ( $\approx 200$  V) and the device is allowed to settle down for a few seconds.

#### 3.2. Relative quantum efficiency

The relative quantum efficiency (RQE) is the ratio of the pulse height at a reduced temperature to the pulse height at room temperature. The RQE is measured by applying a reverse bias of 200 V to the APD, thus producing a unity gain signal (no multiplication). The LED signal is set to a constant amplitude and the pulse height spectrum is taken with the MCA. The center channel of the peak in the spectrum is recorded as the pulse height. The APD is then cooled and the pulse height is recorded as a function of temperature.

<sup>6</sup>RMD Inc., Watertown, MA (private communication).

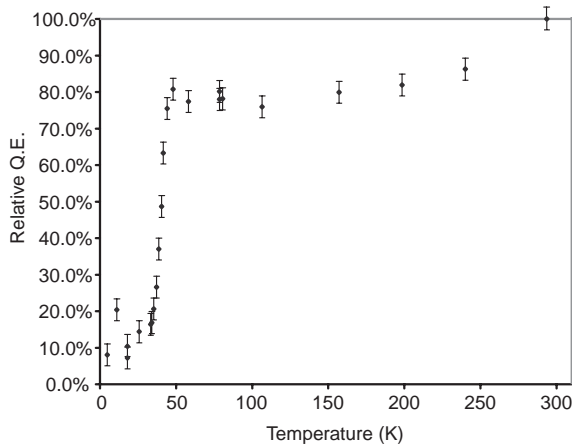


Fig. 3. The relative quantum efficiency of the APD as a function of temperature.

Measurements of the RQE were taken in the temperature range 4.2–300 K and are shown in Fig. 3. The RQE slowly decreases by approximately 20% between 300 and 50 K. Between 50 and 35 K, the RQE drops quickly to approximately 15% of the 300 K value and continues to drop as the APD reaches lower temperatures. We attribute this dramatic drop in RQE to hard carrier freezeout [7]. This drop limits the usefulness of silicon avalanche photodiodes for low-intensity optical photon detection at temperatures below 40 K.

### 3.3. Sensitivity of the APD at low signal levels and temperatures

As stated earlier, our interest in APDs arose from the possibility of using them to detect pulses of 20–30 photons arising from scintillations in liquid helium. After determining that the APD cannot be used for this purpose below 40 K due to premature apparent breakdown and poor quantum efficiency, sensitivity measurements were performed at 77 K.

An absolute calibration of the detection electronics is initially performed using two different methods. First, the APD is operated at a known gain and illuminated with 5.9 keV X-rays from the  $^{55}\text{Fe}$  source. The energy required to produce an electron–hole pair in Si is 3.6 eV, therefore a total

of  $1.6 \times 10^3$  photoelectrons are produced. These electrons are multiplied in the gain region of the APD and sent to the detection electronics. A pulse height spectrum is recorded using the multi-channel analyzer, with the peak arising from the X-ray source. The X-ray source is then replaced with the LED and its output is adjusted so that the peak of the spectrum coincides with the peak from the X-ray source. In this way, the number of photons absorbed by the APD is known. The light from the LED can then be attenuated using neutral density filters to reduce the number of photons per pulse to the desired number.

In the second calibration method, a series of square voltage pulses of either 1 or 2 mV with a period much longer than the 300  $\mu\text{s}$  decay time of the charge preamplifier is applied to a 2 pF capacitor which is connected to the input of the charge-sensitive preamplifier. The channel at which the pulses appear on the MCA coupled with the known charge input determines the calibration of channel number to electrons input into the preamplifier. These two calibration methods agree with each other to within 10%.

The sensitivity measurements proceed as follows. The APD is biased at 200 V to produce a unity gain at 300 K. The LED is biased such that the center channel of the peak on the MCA is well above the device noise. The calibrations described above combined with the manufacturer's room temperature absolute quantum efficiency specification (65% in the green and 75% in the near infrared) allows the number of photons per pulse to be determined. The APD is then cooled to 77 K and pulse height spectra are taken on the MCA for various levels of light input. Due to the non-linear response of the LED to bias voltage, the intensity of the light was varied using neutral density filters. Spectra were taken using filters with optical densities of 1.0 (10% attenuation), 2.0 (1%), and 3.0 (0.1%). To optimize the system for pulse detection, the noise in the detection electronics is minimized and then the reverse bias voltage (and hence the gain) is increased until the dark current noise is approximately equal to the noise from other sources.

Pulses of approximately 30 photons were generated by the LED using a bias supply which

produced 0.5  $\mu\text{s}$  long pulses at a repetition rate of 5 kHz for 10 s. Measurements taken at 77 K determined that the RQE is  $(79 \pm 1)\%$  (again, relative to the 300 K value). The error arises from the uncertainty in pulse height measurements. Combining this value with an estimate of the absolute quantum efficiency in the red at 300 K from the manufacturer's specifications ( $(70 \pm 5)\%$ ) results in an absolute quantum efficiency of  $(55 \pm 4)\%$  at 77 K. From uncertainties in data acquisition, temperature, and applied voltage, we estimate a 10% systematic uncertainty in the APD gain used in this measurement ( $\approx 1000$ ).

A typical pulse height spectrum is shown in Fig. 4. The peak corresponds to  $(30 \pm 4)$  photons incident on the detector and  $(16 \pm 2)$  photons detected. In this graph the APD is operating at a gain of  $1000 \pm 100$ . Pulses of  $(30 \pm 4)$  photons at a 5 kHz repetition rate can be discriminated from the background with approximately 50% efficiency and a signal-to-noise ratio of 15. Higher discrimination thresholds yield even higher signal-to-noise ratio. For example, a signal-to-noise ratio of over 300 is achieved when the efficiency of detection is reduced to 10%. Higher efficiencies can also be achieved if the discrimination level is chosen to be lower, but inconsistencies in our dark count data prevent meaningful analysis at these lower discrimination levels.

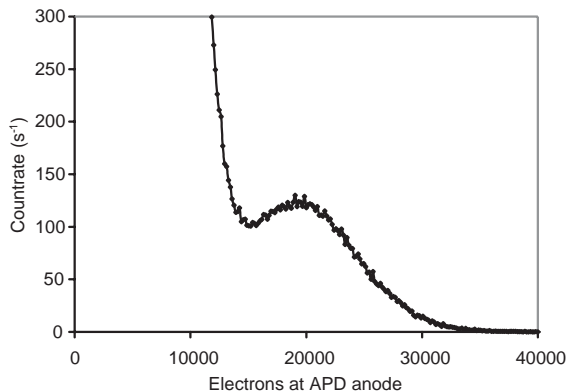


Fig. 4. A typical MCA spectrum of APD at 77 K illuminated with a red LED generating 30 photon pulses.

#### 4. Discussion

The type of APD we tested is manufactured through deep diffusion of p-type silicon onto n-type substrate. Its proper operation relies on the ability of its depletion region to sustain high electrical field without breaking down. A breakdown occurs when the internal gain of the APD reaches infinity. At high temperatures  $\geq 100$  K, all dopant impurities are thermally ionized. The multiplication process begins only when an initial carrier gains enough energy (3.6 eV) to create additional electron–hole pairs in the silicon lattice. As the temperature of the device is lowered, the mobility of carriers increases as phonon scattering is reduced. At the same reverse biasing, the carriers gain more energy before they collide with lattices. As a result, the breakdown voltage decreases with temperature [8]. At even lower temperatures, when carriers start to freeze out at impurity sites, the width of the depletion region grows thicker and neutral impurities begin to form in the depletion region. For typical dopants, the impurity ionization energies are on the order of 0.05 eV. Although the electrical field is decreased, the carrier multiplication process begins at considerably lower reverse biasing, which explains the premature breakdown phenomenon we observed.

The abrupt changes in relative quantum efficiency at the same temperature regime suggest that it could be closely related to the carrier freeze-out. A possible explanation is the increase in hole–electron recombination probability as the depletion zone becomes thicker. In order to have a complete understanding of the APD behavior at these low temperatures more experimental investigations are needed.

In general, carrier freeze-out is a problem for all silicon-based APDs at very low temperatures. The exact behavior will depend on the type of dopants and the amount of doping. To alleviate the problem, one can use dopants with shallower impurities levels. APDs fabricated with Ge or InGaAs will be less affected by carrier freeze-out, because of their shallower impurity levels. However, the gain achieved by existing Ge or InGaAs APDs are considerably lower than silicon APDs.

## 5. Conclusion

For temperatures around 77 K, large-area APDs can be used to discriminate scintillation pulses of approximately 30 photons from the background with high efficiency and low background rate. In experiments where the detection of scintillation in cryogenic liquids is involved, such as the neutron lifetime experiment, they are a viable option. APDs are not effective below the carrier freeze-out temperature ( $\approx 40$  K).

## Acknowledgements

We acknowledge helpful conversations with Richard Farrell of RMD, Inc., and Larry Lapson of Harvard University Department of Chemistry. We thank Prof. M. Snow of Indiana University for lending us the test cryostat. This work is supported in part by the National Science Foundation under grant number PHY-0099400.

## References

- [1] J.M. Doyle, S.K. Lamoreaux, *Europhys. Lett.* 26 (1994) 253.
- [2] P.R. Huffman, C.R. Brome, J.S. Butterworth, K.J. Coakley, M.S. Dewey, S.N. Dzhosyuk, R. Golub, G.L. Greene, K. Habicht, S.K. Lamoreaux, C.E.H. Mattoni, D.N. McKinsey, F.E. Wietfeldt, J.M. Doyle, *Nature* 403 (2000) 62.
- [3] V.N. Solovov, V. Chepel, M.I. Lopes, R. Ferreira Marques, A.J.P.L. Policarpo, *Nucl. IEEE Trans. Nucl. Sci.* NS-47 (2000) 1307.
- [4] V.N. Solovov, A. Hitachi, V. Chepel, M.I. Lopes, R. Ferreira Marques, A.J.P.L. Policarpo, *Nucl. Instr. and Meth. A* 488 (2002) 572.
- [5] N.G. Woodard, E.G. Hufstedler, G.P. Lafyatis, *Appl. Phys. Lett.* 64 (1994) 1177.
- [6] J.J. Fox, N.G. Woodard, G.P. Lafyatis, *Rev. Sci. Instrum.* 70 (1999) 1951.
- [7] E.A. Gutiérrez-D., M.J. Deen, C. Claeys, *Low Temperature Electronics: Physics, Devices, Circuits, and Applications*, Academic Press, London, UK, 2001, p. 56.
- [8] K. Seeger, *Semiconductor Physics (An Introduction)*, Springer, Berlin, Germany, 1985, p. 296.